

Cone and rod photoreceptor transplantation in models of the childhood retinopathy Leber congenital amaurosis using flow-sorted Crx-positive donor cells

J. Lakowski^{1,†}, M. Baron^{1,†}, J. Bainbridge^{2,3}, A.C. Barber², R.A. Pearson², R.R. Ali^{2,*} and J.C. Sowden^{1,*}

¹Developmental Biology Unit, UCL Institute of Child Health, University College London, 30 Guilford Street, London WC1N 1EH, UK, ²Department of Genetics, UCL Institute of Ophthalmology, University College London, Bath Street, London EC1V 9EL, UK and ³Vitreoretinal Service, Moorfields Eye Hospital, London EC1V 2PD, UK

Received July 18, 2010; Revised and Accepted August 30, 2010

Retinal degenerative disease causing loss of photoreceptor cells is the leading cause of untreatable blindness in the developed world, with inherited degeneration affecting 1 in 3000 people. Visual acuity deteriorates rapidly once the cone photoreceptors die, as these cells provide daylight and colour vision. Here, in proof-of-principle experiments, we demonstrate the feasibility of cone photoreceptor transplantation into the wild-type and degenerating retina of two genetic models of Leber congenital amaurosis, the *Crb1*^{rd8/rd8} and *Gucy2e*^{-/-} mouse. Crx-expressing cells were flow-sorted from the developing retina of CrxGFP transgenic mice and transplanted into adult recipient retinæ; CrxGFP is a marker of cone and rod photoreceptor commitment. Only the embryonic-stage Crx-positive donor cells integrated within the outer nuclear layer of the recipient and differentiated into new cones, whereas postnatal cells generated a 10-fold higher number of rods compared with embryonic-stage donors. New cone photoreceptors displayed unambiguous morphological cone features and expressed mature cone markers. Importantly, we found that the adult environment influences the number of integrating cones and favours rod integration. New cones and rods were observed in ratios similar to that of the host retina (1:35) even when the transplanted population consisted primarily of cone precursors. Cone integration efficiency was highest in the cone-deficient *Gucy2e*^{-/-} retina suggesting that cone depletion creates a more optimal environment for cone transplantation. This is the first comprehensive study demonstrating the feasibility of cone transplantation into the adult retina. We conclude that flow-sorted embryonic-stage Crx-positive donor cells have the potential to replace lost cones, as well as rods, an important requirement for retinal disease therapy.

INTRODUCTION

Human vision relies mainly on cone photoreceptors, the majority of which reside in the fovea of the central retina. Away from the fovea, rods outnumber cones by a ratio of about 30:1. Cone photoreceptors mediate colour and daylight vision as well as high visual acuity, whereas rod photoreceptors are responsible for dim light vision. Cone and rod photoreceptors differ

significantly in their biochemical and structural properties as well as their synaptic connections (Fig. 1C). Diseases that result in the loss of the cone photoreceptor type, such as Leber congenital amaurosis (LCA), age-related macular degeneration, and various kinds of inherited rod and cone retinal degenerations, consequently lead to severe visual impairment or blindness (1). More than 150 different genes causing inherited retinal disease

*To whom correspondence should be addressed. Tel: +44 2079052121; Fax: +44 20778314366; Email: j.sowden@ich.ucl.ac.uk (J.C.S.); Tel: +44 2076086817; Email: r.ali@ucl.ac.uk (R.R.A.)

†The authors wish it to be known that, in their opinion, the first two authors should be regarded as joint First Authors.

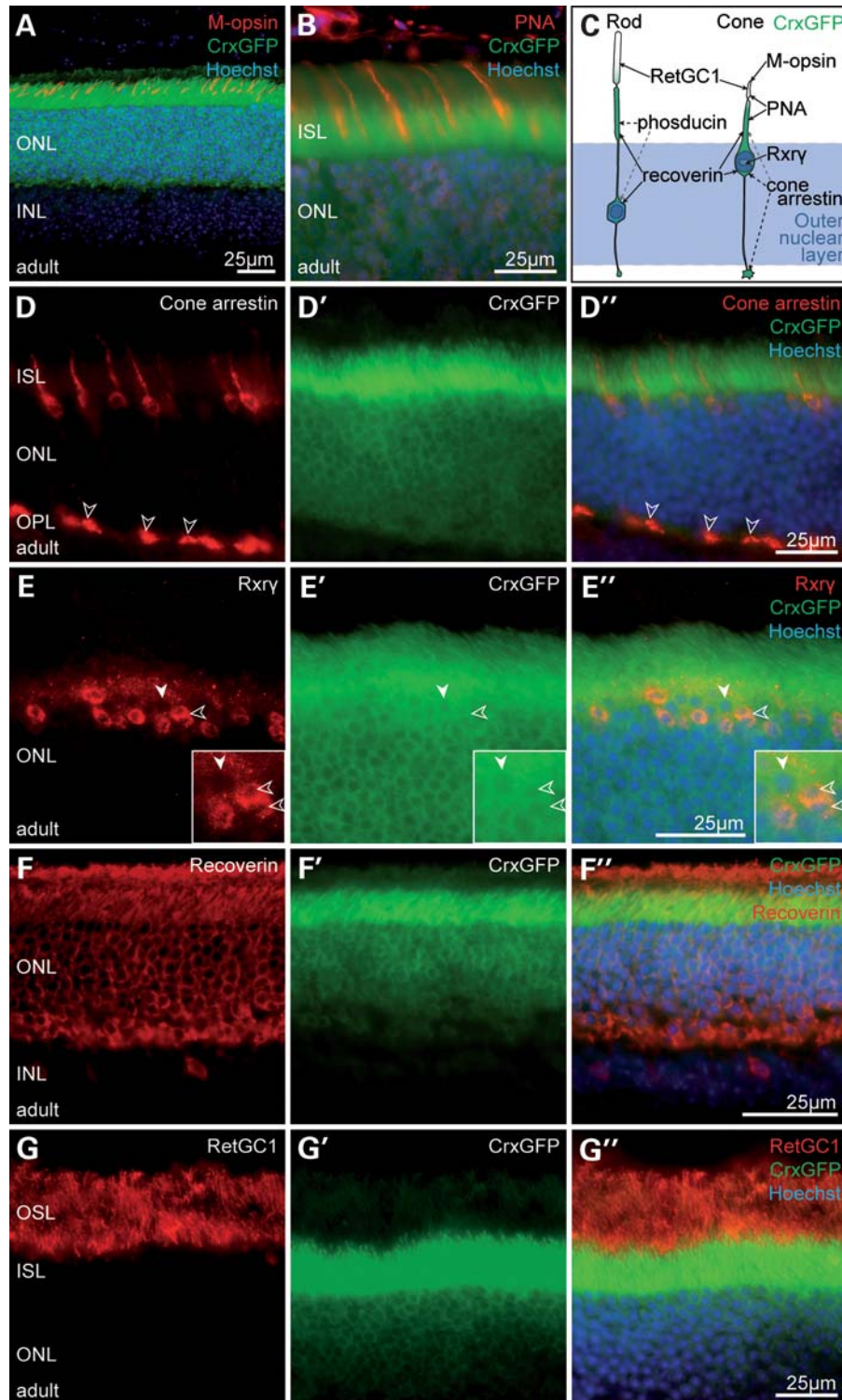


Figure 1. The CrxGFP transgene is expressed in both rod and cone photoreceptors. (A, B, D–G) Immunostaining of CrxGFP adult retina. (D–G) Target protein immunostaining (red); (D'–G') CrxGFP labelling (green); (D''–G'') three channels merge with Hoechst nuclear stain (blue). CrxGFP co-localizes with the cone photoreceptor markers, medium wavelength (M)-opsin (A), the lectin peanut agglutinin (PNA) (B), cone arrestin (D) and retinoid X receptor gamma (Rxry) (E). CrxGFP cells also co-label with the general mature photoreceptor markers recoverin (F) as well as retinal guanylate cyclase 1 (RetGC1/Gucy2e) (G). Double-labelled photoreceptors (D', E') exhibit characteristic cone morphologies with polymorphic nuclei near the outermost edge of the ONL (E, insets, open arrowheads) and large cone pedicles in the OPL (D, open arrowheads). (C) A cartoon representation of rod and cone photoreceptor morphology and marker expression. (A) is a confocal z-projection. ONL, outer nuclear layer; INL, inner nuclear layer; ISL, inner segment layer; OPL, outer plexiform layer.

have been identified (www.sph.uth.tmc.edu/Retnet/). While the majority of genes associated with retinal degeneration are rod photoreceptor-specific, it is the eventual loss of the cones owing to the interdependence of both photoreceptor types that causes the loss of visual acuity (2).

Since photoreceptor death is an irreversible process, it accounts for a large proportion of worldwide blindness and is the leading cause of blindness in developed countries. As no effective treatment is currently available to restore lost photoreceptors or visual function, photoreceptor transplantation as a therapeutic approach for genetic retinal disease has been a long-standing goal (3,4). Photoreceptor transplantation offers the prospect of replacing cells lost through disease, restoring light sensitivity and providing photoreceptor cells lacking deleterious gene mutations. In an effort to identify a transplantable cell population, we recently demonstrated that rod precursor cells can integrate into the adult or degenerating mouse retina when taken from the developing retina at a time coincident with the peak of rod genesis (5). We found that sub-retinally transplanted rod precursors integrated specifically into the outer nuclear layer (ONL) of the host and developed into functional rod photoreceptors, forming synaptic connections in their new environment. Furthermore, we observed an improved low-light visual function by transplanting wild-type cells in a genetic model of severe retinal degeneration, the rhodopsin knockout (*Rho*^{-/-}) mouse. Transplantation of genetically tagged cells expressing the rod transcription factor *Nrl* (neural retina leucine zipper) demonstrated that integrated rods arose only from immature, yet post-mitotic, rod precursors and not from proliferating retinal progenitor cells (RPCs) or stem cells (5). This study did not investigate cone transplantation. Recently, it was shown that transplantation of a mixed population of retinal cells derived by *in vitro* differentiation of human embryonic stem cell (ESC) gave rise to rod photoreceptors after transplantation into the mouse retina (6). Previous studies (5,6) provide strong evidence that the adult retina is a permissive environment for rod photoreceptor integration and development of new functional rod photoreceptors, establishing the basis for future photoreceptor cell replacement therapy for a number of retinal diseases.

Although these reports represent important steps towards a possible treatment for retinal disease, they do not address the necessity to replace the lost cone photoreceptors crucial to human visual function. It is therefore critical to explore the potential of cell-based retinal-repair strategies for cone photoreceptor replacement and to define the type of donor cell population that is able to generate both cone and rod photoreceptor following transplantation. We hypothesized that the ontogenetic stage of donor cells will be important for cone transplantation, though this has not yet been investigated. Sub-retinal transplantation of cultured RPCs into *Rho*^{-/-} mice did not give rise to new rods in the ONL, but one cell immunolabelling for cone opsin was reported (7). Lamba *et al.* (6) reported intravitreal transplantations of human ESC-derived retinal cells into neonatal mice; these donor cells integrated into all retinal layers and immature S-opsin labelling cells were described lacking inner or outer segments. No study to date has demonstrated mature cone morphology or conclusive evidence of new cone cell differentiation and integration into the ONL following transplantation

into the adult retina and there is no published data on the frequency of cone cell differentiation and integration after transplantation.

During retinal histogenesis, seven different cell types are generated in sequential but overlapping steps from multipotential RPCs, a process that is highly conserved throughout vertebrate evolution (8–11). In mice, cone photoreceptors are born (become post-mitotic) early, commencing at embryonic day E10 with the peak soon after (~E14–15), while rod photoreceptor birthing happens over a much longer period of time with the peak in the early postnatal period (12). The final specification of the photoreceptor subtypes by expression of the corresponding opsin genes and mosaic patterning is significantly delayed to postnatal day (P)4–13, suggesting a degree of plasticity in cell fate (1). Generation of photoreceptors in vertebrates is coordinated by the paired-type homeodomain transcription factors *Otx2* (orthodenticle homeobox 2) and *Crx* (cone rod homeobox) (13–16). *Crx* is one of the earliest known photoreceptor markers, regulating development of rods and cones (17) and interacts with other transcription factors and co-regulators (18). Rod photoreceptors are specified by the concerted interaction of *Crx* with *Nrl* (13,19) and the nuclear orphan receptor *Nr2e3* (18). Although cone development is not well understood, the retinoic acid receptor (*Rar*) and retinoid X and orphan receptor (*Rxr* and *Ror*) families, in particular, are of critical importance for the generation of the various cone subtypes (20–22). The importance of the *Crx* gene in ontogenesis is underlined by several severe human ocular conditions, including LCA (23), autosomal-dominant cone–rod dystrophy (24) and autosomal-dominant retinitis pigmentosa (23), all of which can occur as a direct result of *CRX* mutation. Similarly, homozygous *Crx* knockout mice lack photoreceptor function and are born blind, recapitulating some human phenotypes (25). Taken together, *Crx* is indispensable for normal development of the visual system in humans and other mammals.

In this study, we present the first clear evidence for the transplantation of mouse cone photoreceptors, which has not been demonstrated previously. We utilized a new *CrxGFP* transgenic mouse line (26) that labels all post-mitotic developing and mature cone and rod photoreceptors. By flow-sorting immature *Crx*-expressing cells from various developmental time points and transplanting the genetically labelled populations into wild-type or degenerating mouse retinas, we were able to compare their integration competency and ability to generate cones after transplantation. We show in the proof-of-principle experiments that embryonic-stage *Crx*-expressing precursor cells migrate into the adult host ONL after transplantation and generate new cones, as well as rods. Newly generated cones displayed the distinctive morphological, positional and immunohistochemical characteristics of mature cone photoreceptors. This is the first time the behaviour of flow-sorted photoreceptor precursor populations has been compared from different developmental stages. We find that integration of rod photoreceptors is 10-fold more efficient using postnatal *CrxGFP* donor cells compared with embryonic stage donors and up to 15 000 new photoreceptors were observed, 10-fold higher than previous work (5). Importantly, we found that the host environment influences the number of integrating cone cells and favours rod cell integration in line with the normal bias of rods over cones in the adult retina

(35:1). We show that the ratio of newly integrated cone to rod cells is similar to that found in the wild-type adult retina. Moreover, transplantation of embryonic-stage *Crx*-expressing donor cells into a cone-deficient retina, the *Gucy2e*^{-/-} model of LCA, resulted in a higher proportion of cones among the total number of integrated photoreceptor cells. This effect was not observed in a second model of LCA, the *Crb*^{rd8/rd8} retina indicating that cone depletion creates a more optimal environment for cone transplantation, which may be relevant for macular repair strategies. Our findings demonstrate for the first time that transplantation of flow-sorted *Crx*-positive embryonic-stage cells generates new cone photoreceptors in two models of LCA and present a useful model for further investigation towards cone cell replacement therapy.

RESULTS

The *CrxGFP* transgene labels developing cone and rod photoreceptors

In normal mouse development, *Crx* expression commences around embryonic day (E) 12 in the neural retina (17). In the *CrxGFP* transgenic line, GFP-expressing cells were first detectable at E13.5 and were predominantly located adjacent to the ventricular surface (Supplementary Material, Fig. S1A, arrowheads). GFP expression increased throughout embryonic and early postnatal development in cells located at the outer aspect of the neuroblastic layer, the site of newly born photoreceptor cells (Supplementary Material, Fig. S1B–D). By P3, GFP expression was present in photoreceptor cells of the nascent ONL, which was around five cells thick (Supplementary Material, Fig. S1D). GFP-positive cells were not labelled with the mitotic cell marker phospho-histone H3 (Supplementary Material, Fig. S1E) consistent with previous reports indicating that *Crx* is expressed in post-mitotic cells (27). These data and the recently published characterization of this transgenic line (26) indicate that the *CrxGFP* faithfully labels newly born and developing photoreceptor precursor cells.

Expression of the nuclear retinoid X receptor gamma gene (*Rxry*) during development is necessary to establish the S-opsin gradient in cone photoreceptors (20). Though there are no known markers that discriminate between immature rods and cones in mouse retinae, *Rxry* has been proposed to be an early cone marker based on its expression pattern in post-mitotic cones (20). Here, we found in the developing *CrxGFP* retina that *Rxry* co-labelled a fraction of GFP-expressing photoreceptors consistent with a marker of developing cone cells (Supplementary Material, Fig. S1A–D). At E15.5, the majority of GFP-positive cells (~75%) expressed high levels of *Rxry* (Supplementary Material, Fig. S1B), in line with the classic cell-birthing studies using tritiated-thymidine, which concluded that most cone photoreceptors are born around E14.5 (12). At subsequent developmental stages, the percentage of *Rxry*-positive cells among the *Crx*-expressing cell population decreased progressively (62% at E17.5; Supplementary Material, Fig. S1C), reflecting the gradual increase in rod genesis that peaks around birth. At P3, the ratio of *Rxry*/GFP cells approached levels observed in the adult retina and did not change thereafter (Supplementary Material, Fig. S1D). Previously, *Rxry* was shown to be

specifically expressed in all cones by P5 and to persist in adult cones (20).

In the adult retina, *CrxGFP* is expressed throughout the ONL. A subset of *CrxGFP* cells co-localized with *Rxry*, in addition to other markers of mature cone photoreceptors, such as M-opsin, the lectin peanut agglutinin and cone arrestin (*Arr3*) (Fig. 1A–E). By contrast, all *CrxGFP* cells were labelled with the general photoreceptor markers recoverin and retinal guanylate cyclase 1 that are expressed in both rods and cones (Fig. 1F and G).

It is known that rod and cone photoreceptors in rodents differ significantly in their nuclear morphology (12). In agreement, we found that cone photoreceptors located at the outermost edge of the ONL (Fig. 1D and E) and expressing cone arrestin and *Rxry* displayed a conventional nuclear configuration with several heterochromatin foci (Fig. 1E and inset; open arrowheads), while rod photoreceptors contained one single heterochromatin centre (Fig. 1E and inset; solid arrowheads). Together, these data confirm that the *CrxGFP* transgene recapitulates normal *Crx* expression as previously reported (13,17,26) and labels post-mitotic photoreceptor precursor cells as well as mature cone and rods cells.

Transplanted *CrxGFP* photoreceptor precursors integrate into the adult wild-type retina

To test the transplantation potential of *Crx*-expressing photoreceptor precursors from successive developmental time points, we harvested GFP-positive retinal cells from *CrxGFP* mice and transplanted them into the sub-retinal space of adult wild-type recipients. Previously, we demonstrated that transplanted immature retinal cells, harvested by dissociation of the neural retina shortly after birth, achieved successful rod photoreceptor transplantation in mice (5). However, the feasibility of transplanting cone cells has not been explored so far. We hypothesized that immature photoreceptors taken from the embryonic retina, especially around the time of cone genesis, would have the highest cone transplantation potential. As *CrxGFP* labels both rod and cones cells, use of this transgene allowed us to investigate the integration efficiency of both photoreceptor types simultaneously, using donor cells isolated from different ontogenetic stages.

Retinae derived from *CrxGFP* donor embryos (E12.5, E14.5, E15.5, E16.5, E17.5) or postnatal mice (P2, P3) were dissociated and cells sorted based on GFP fluorescence. Equal numbers of flow-sorted cells expressing the *CrxGFP* transgene from each developmental stage were transplanted into the recipient retina. Three weeks after transplantation, a large number of GFP-expressing cells had migrated into the ONL (Fig. 2A and B). The spread of the integrated cells along the ONL correlated with the initial, temporary retinal detachment from the RPE. Cell integration was restricted to the ONL and we never observed GFP-positive cells in other retinal cell layers. GFP-positive cells in the ONL exhibited morphological features of mature photoreceptors including inner and outer segments, and synapses in the OPL (Fig. 2A and B solid and open arrowheads, respectively).

Samson *et al.* (26) described *CrxGFP* expression in bipolar cells and we also noted weak expression in the inner nuclear layer of the adult retina where bipolar cells reside

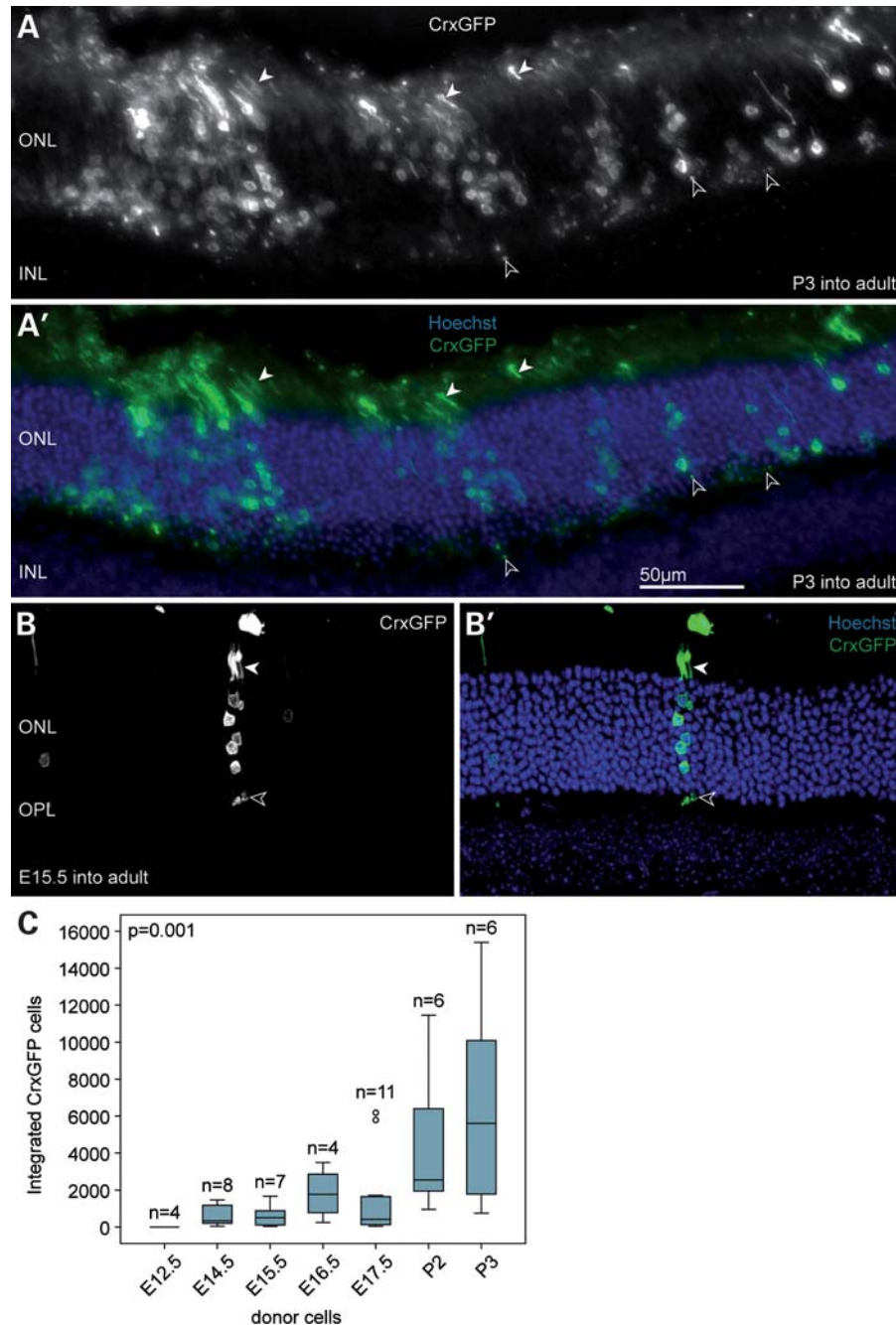


Figure 2. The majority of transplanted CrxGFP cells develop into rod photoreceptors in the adult wild-type retina. **(A)** Clusters of transplanted P3 CrxGFP donor cells (green) migrated into the host ONL near the injection site. Cells exhibit typical rod photoreceptor morphology with highly condensed heterochromatin pattern, slender inner and outer segments (closed arrowheads) and spherical synapses (open arrowheads) in the OPL. **(B)** Transplanted E15.5 CrxGFP cells integrated into ONL and were usually observed as single- or small groups of photoreceptors. **(C)** Number of integrated CrxGFP cells per retina displayed in relationship to donor age. A trend was observed with significantly more cells integrating into the ONL with increased donor cell age (Spearman correlation, $P < 0.01$). Horizontal bars indicate the median value. **(B)** is a confocal z-projection. All retinæ were examined 3 weeks post-transplantation. ONL, outer nuclear layer; INL, inner nuclear layer; OPL, outer plexiform layer. Hoechst nuclear stain (blue).

(Supplementary Material, Fig. S2A). As immature CrxGFP-positive bipolar cells could be present in the flow-sorted CrxGFP donor populations, we performed immunostaining using the bipolar markers, Protein kinase C α (PKC α) and Chx10 to test for new integrated bipolar cells. Integrated bipolar cells were not observed. PKC α and Chx10-positive

CrxGFP cells were observed only in the sub-retinal space (Supplementary Material, Fig. S2B–D), suggesting that in transplantation experiments, bipolar cells were not able to migrate into the adult retina.

Integrated CrxGFP cells with photoreceptor morphology were observed at all except the earliest (E12.5) developmental

time points we tested. The overall integration efficiency of the *Crx*-positive cells depended on the stage from which the *CrxGFP* donor cells had been derived (Supplementary Material, Fig. 2C). In all transplant experiments, clusters of *CrxGFP* cells survive in the sub-retinal space and the RPE remains detached at sites adjacent to the clusters (Supplementary Material, Figs S3 and S5C). We assume that either these cells do not have optimal integration properties or create their own microenvironment that limits integration. Typical integration values from the embryonic donor populations varied between several hundred to a few thousand cells (median for E14.5 donors = 334 *CrxGFP* cells; range of total number of integrated *CrxGFP* cells per retina = 42–1466), whereas the postnatal donor populations gave rise to up to 15 000 integrated photoreceptor cells (median for P3 donors = 5610; range of total number of integrated *CrxGFP* cells per retina = 754–15 402), ~7.5% of the total number of cells transplanted. Using a bivariate statistical analysis, we found that the correlation between the increase in *CrxGFP* donor age and the amount of integrated GFP-expressing photoreceptors was highly significant ($P < 0.001$) (Supplementary Material, Fig. 2C). These data show that postnatal *CrxGFP* photoreceptor precursors have an ~10-fold higher integration efficiency compared with embryonic ones. Because the number of transplanted *CrxGFP* cells, as well as the age and type of recipient animals remained constant in these experiments, we suppose that this difference in integration efficiency reflects a temporal change in the properties of the transplanted *CrxGFP* cell population.

To verify that the *Crx*-positive photoreceptors, which integrated in the host ONL had originated from cells that had already undergone terminal mitosis at the time of grafting, we performed bromodeoxyuridine (BrdU) labelling of the transplanted cells. Following the transplantation of P2 *CrxGFP* donor cells, the recipient animals received a daily intraperitoneal injection of BrdU for a period of 1 week. As expected, 3 weeks later, none of the integrated *CrxGFP*-expressing photoreceptors in the host ONL had incorporated BrdU, indicating that they had exited the cell cycle prior to transplantation. Rarely, we observed BrdU-positive/GFP-negative cells in the sub-retinal space of recipients suggesting that a few RPCs were included in the transplanted cell population (Supplementary Material, Fig. S3, open arrowheads).

Transplanted *CrxGFP* photoreceptor precursors develop into rods and cones

The majority of transplanted *CrxGFP* cells that integrated into the host ONL displayed the unambiguous morphology of mature rod photoreceptors including spherical synapses, a condensed nuclear heterochromatin configuration and correctly oriented inner segments (Fig. 3A–D). Photoreceptor outer segments were also observed in transplanted cells (Fig. 3C, arrowheads). Furthermore, all integrated cells were in proper alignment with the host photoreceptors, while their cell bodies were found at differing positions across the depth of the host ONL (Fig. 3A–D). As expected, these cells also labelled for the rod-specific phototransduction cascade component, phosducin (Fig. 3A), in addition to expressing

pan-photoreceptor markers such as recoverin and retinal guanylate cyclase-1, but not the cone marker *Rxr γ* (Fig. 3B–D). The synapses of integrated *CrxGFP* photoreceptors also labelled for the synaptic markers, Bassoon and Dystrophin, and immunostaining with the bipolar marker *PKC α* showed close association between the bipolar cell dendrite and the rod spherule (Supplementary Material, Fig. S4).

We next assessed if the transplanted *CrxGFP*-expressing precursors gave rise to mature cone photoreceptors after transplantation into adult wild-type retinæ. We used immunostaining of the *CrxGFP*-integrated cells by the cone marker *Rxr γ* to determine the relative proportion of mature rods and cones derived from donor populations at each developmental stage. In particular, we were interested in how the developmental stage of the donor cells affected cone integration efficiency. Although, rods vastly outnumber cone photoreceptors in the mouse retina, we predicted that the *Crx*-expressing donor populations from early retinal development would contain a comparatively high proportion of cone precursors, as most rods are born relatively late.

We observed GFP/*Rxr γ* -positive cells displaying characteristic cone profiles with all integration competent embryonic donor populations (Fig. 4A–C). The presumed cones were without exception located in the outer aspect of the ONL, aligned with the host cone cells, possessed a short inner- and outer segment and frequently showed the characteristic large cone pedicle in the outer plexiform layer (Fig. 4A–C, open arrowheads). Confocal microscopy also showed the outgrowth of telodendria from cone pedicles, structures that are usually associated with gap junctions between neighbouring photoreceptors, suggesting that the transplanted cells were connecting with the host retinal circuitry (see Supplementary Material, Video S1). The cells were also immunopositive for cone arrestin, a second pan-cone marker (Fig. 4D). The typical nuclear heterochromatin pattern of photoreceptors is usually not established before postnatal day 28 (28). As a rule, the observed cells always displayed a distinct multi-focal heterochromatin arrangement (Fig. 4A–D; right hand inset) further corroborating their mature cone identity.

As hypothesized, a higher proportion of cone cells was observed among the total number of integrated photoreceptor cells using the embryonic donor cells when compared with postnatal donor cells (Fig. 4E). The highest contribution of cone cells expressing both GFP and *Rxr γ* to the overall number of integrated photoreceptors was observed with E14.5 donors (median 0.76%; range of number of cones observed per retina = 0–10; Fig. 4E). At all time points, the median level of rod integration was at least 100-fold greater than that of cones (*Rxr γ* -negative, GFP-expressing population; Fig. 4E). The highest total number of integrated cones observed was 54 cells using E17.5 donor cells (median 0.35% *Rxr γ* /GFP; range of total cone number 0–54). By contrast, cone cells were very rarely found when P3 donor cells were used. We found that cone integration efficiency was inversely correlated with increased age of the *CrxGFP* donor cells ($P = 0.001$; Fig. 4E). These data indicate that while both embryonic and postnatal *CrxGFP* donor cells effectively integrate into the mature ONL and differentiate into mature photoreceptors, there are clear stage-specific differences between the transplantation potential of the photoreceptor

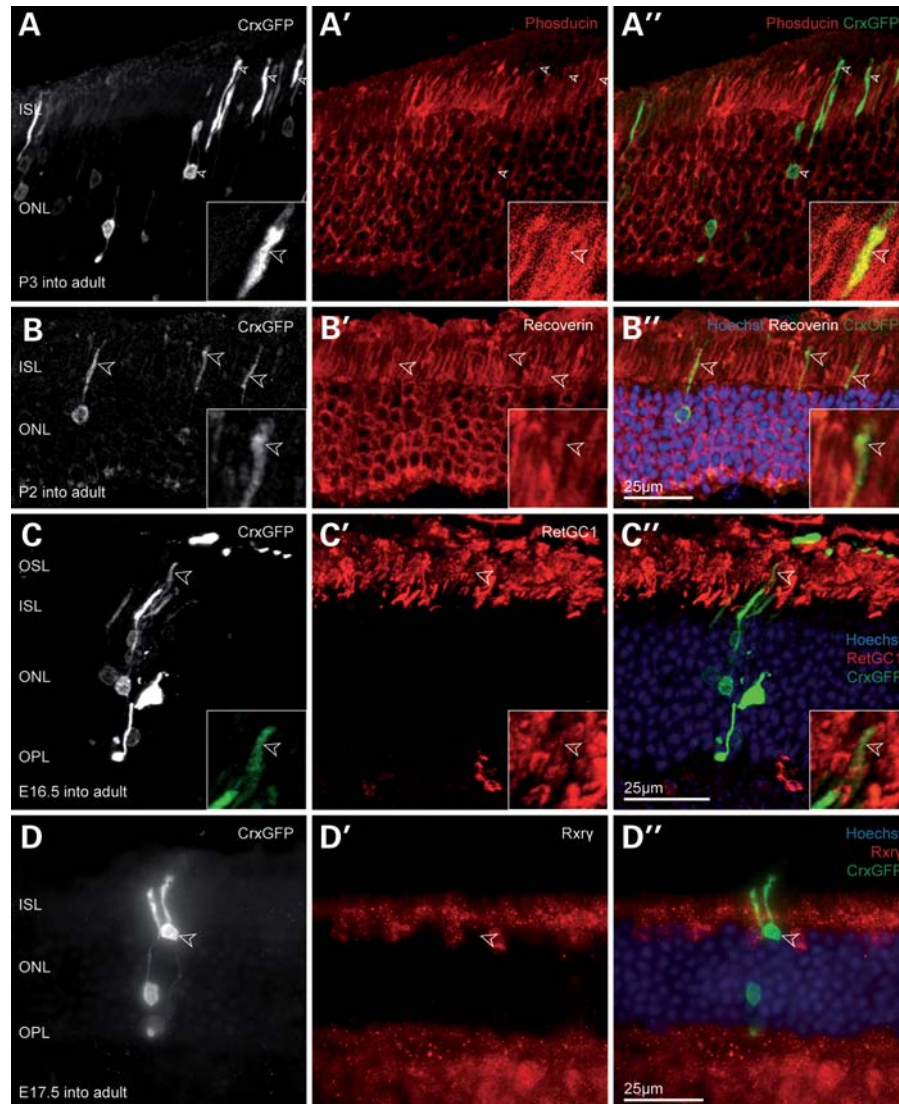


Figure 3. Transplanted CrxGFP cells with rod morphology co-label for functional photoreceptor markers. (A–D) CrxGFP labelling (grey scale), A'–D' target protein immunostaining (red), A''–D'' three channels merge with CrxGFP (green) and Hoechst nuclear stain (blue). (A) Transplanted CrxGFP cells co-express the rod marker phosducin in inner segments and the cell body (arrowheads). Insets show a higher magnification and single optical section showing co-localization in the inner segment. (B) The general photoreceptor marker recoverin is expressed in transplanted CrxGFP cells. Arrowheads highlight inner segments. Insets show a higher magnification and single optical section showing co-localization in the inner segment. (C) Retinal guanylate cyclase 1 (RetGC1/Gucy2e) is expressed in the outer segments of transplanted rod photoreceptors (arrowheads). Insets display a higher magnification of the outer segment. (D) Transplanted cells with rod morphology do not co-label for the cone marker Rxry. All retinae were examined 3 weeks post-transplantation. (A–C) are confocal z-projections. ISL, inner segment layer; ONL, outer nuclear layer; OSL, outer segment layer; OPL, outer plexiform layer.

sub-populations. The postnatal *Crx*-positive donors are more efficient and give rise to higher numbers of new rod photoreceptors than the embryonic donors. Yet, the embryonic donors more readily give rise to cone photoreceptors.

Rxry-expressing embryonic precursor cells generate cones during retinal development

Rxry staining (Supplementary Material, Fig. S1) and classical photoreceptor cell birth dating studies (12) indicate that the majority of CrxGFP cells present in the developing retina (>75% at E15.5) are cone precursors. Rxry immunostaining of flow-sorted CrxGFP populations used for transplant

experiments also showed a high level of co-localization (>80% at E15.5; Supplementary Material, Fig. S5D). As it has not been established when final specification to the cone fate occurs, or if Rxry exclusively labels immature cones in the embryonic retina, we performed BrdU pulse chase analysis of cone photoreceptor development. CrxGFP pregnant females received intraperitoneal BrdU injections at E14 and embryos were analysed for Rxry, BrdU and CrxGFP co-localization at E15.5, P0 and P21 (Supplementary Material, Fig. S6). No significant differences were observed between the time points analysed; at all stages, more than 90% of the CrxGFP/BrdU-positive cells also labelled for Rxry indicating that most of the CrxGFP-positive cells born between E14 and

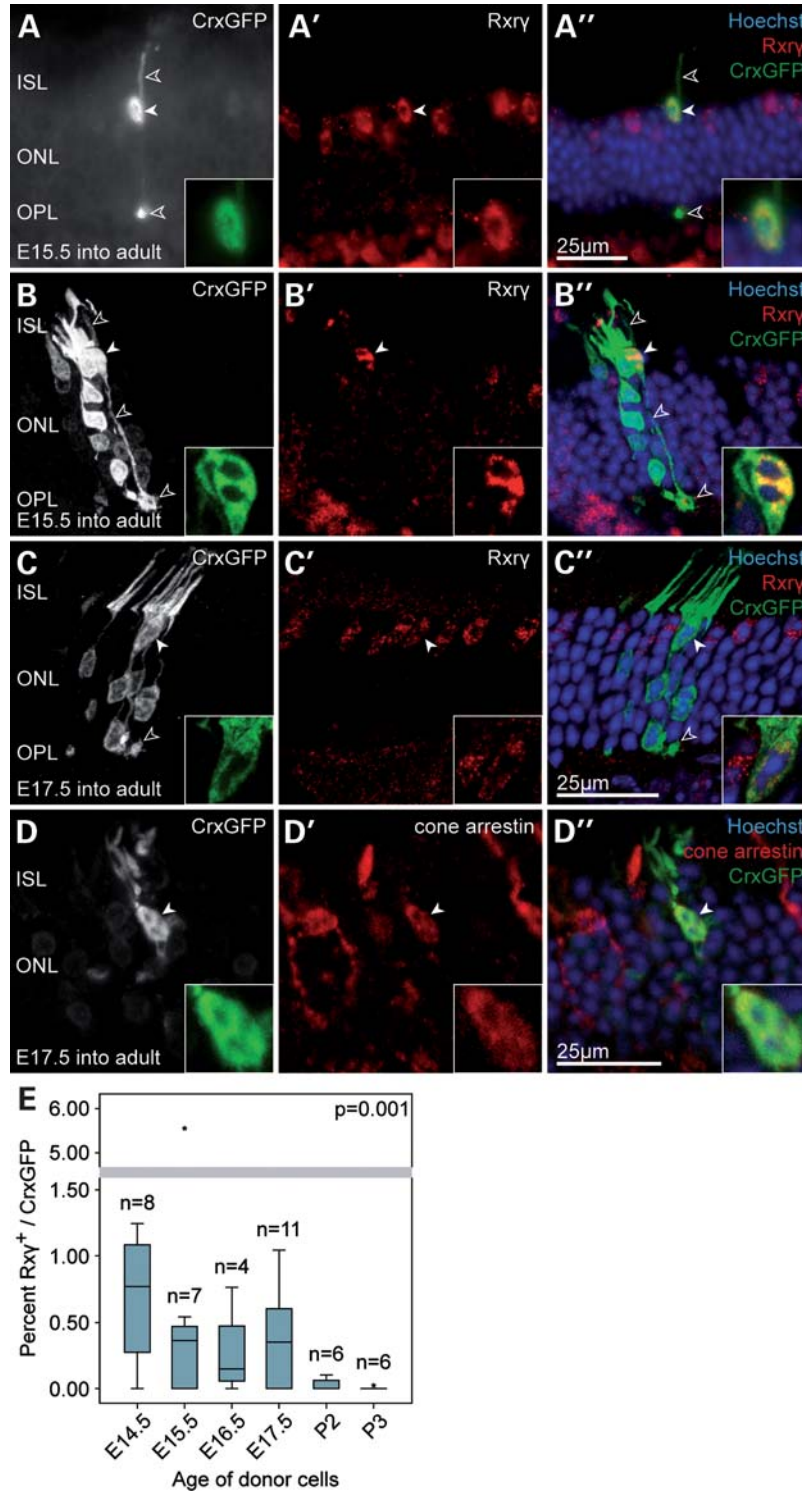


Figure 4. A small number of transplanted embryonic CrxGFP donor cells develop as cone photoreceptors in the wild-type retina. (A–D) A small number of transplanted embryonic CrxGFP precursors migrated into the host ONL from the sub-retinal space and differentiated into cone photoreceptors expressing the cone marker Rxy. Hoechst nuclear stain demarcates ONL in (A''–D''). Presumed cone cell bodies were without exception located at the outer aspect of the host ONL (solid arrowheads and insets), had large cone ribbon synapses (pedicles) in the OPL (open arrowheads) and exhibited a polymorphic heterochromatin structure typical for mature cone photoreceptors (Hoechst nuclear stain in insets). (A'–C') Three examples of cone photoreceptors displaying nuclear Rxy immunostaining (solid arrowheads). (D) Example of a cone photoreceptor co-labelling with cone arrestin. (B'' and C'') Integrated cone cells (green; arrowheads) are located close to several transplanted rod cells (green, without arrowheads), which do not label with Rxy and have typical rod morphologies. (A–D) CrxGFP labelling (greyscale and inset green); (A'–D') Rxy and cone arrestin immunostaining (red); (A''–D'') three channels merge with Hoechst nuclear stain (blue). All retinæ were examined 3 weeks post-transplantation. (B–D) are confocal z-projections. (E) Graph of the efficiency of cone cell integration observed after transplants using CrxGFP donor cells at each donor age. Cone cell efficiency calculated as the proportion of newly integrated photoreceptors that are cones; Rxy CrxGFP double-positive cells/total CrxGFP. A trend was observed with significantly higher cone integration efficiencies observed using embryonic CrxGFP donor cells when compared with postnatal CrxGFP donor cells (Spearman correlation, $P < 0.01$). Horizontal bars indicate the median value. ISL, inner segment layer; ONL, outer nuclear layer; OPL, outer plexiform layer.

E15 are cone precursors expressing *Rxry* (Supplementary Material, Fig. S6). These data show that the majority of embryonic CrxGFP donor cells isolated and tested by transplantation into adult recipients are cone precursor cells that would have developed into cones if left in the developing retinal environment.

Effect of host environment on cone precursor cell integration

Before examining the potential of CrxGFP donor cell transplants into the diseased retina, we considered the influence of the wild-type host environment on the integration behaviour of the transplanted cells. We focused, in particular, on the behaviour of the CrxGFP embryonic donor cells, as they demonstrated cone integration potential.

First, we investigated the possibility that selective cone precursor cell loss occurred following transplantation of CrxGFP cells into the sub-retinal space. We reasoned that if cone precursor cells were more sensitive to the transplantation procedure compared with rods, then this would limit the number of integrated cones that could be achieved. Transplanted, but non-integrated, CrxGFP cells survive in the sub-retinal space of recipients and often form rosettes with inwardly oriented photoreceptor segments (Supplementary Material, Fig. S5A', dashed line). We assessed the proportion of these cells that expressed cone markers. Confocal analysis showed that cells co-expressing CrxGFP and *Rxry* or cone arrestin were readily observed in sub-retinal rosettes ($33 \pm 9.4\%$ of CrxGFP-positive cells co-labelled with *Rxry*; $n = 3$ eyes transplanted with E15.5 donors). These cells also exhibited a cone chromatin pattern (Supplementary Material, Fig. S5, solid arrowheads), indicating that cone cell survival was not a limiting factor.

We also analysed the short-term behaviour of the embryonic Crx-expressing donors soon after transplantation into the adult retina by analysing retinal sections at 4 and 10 days post-transplantation. Specifically, we assessed whether integrating cells initially expressed the cone marker *Rxry*. By 4 days post-transplantation, *Rxry*-positive CrxGFP cells were observed within the outer and inner segment layers of the host retina appearing to migrate towards the ONL ($n = 6$; Supplementary Material, Fig. S7B). By 10 days post-transplantation, mature cone and rods were observed in similar proportions to those at 3 weeks post-transplantation and migrating cells were no longer observed within the inner or outer segment layers.

Together these data show that while transplanted *Rxry*-positive cone precursors are present in the sub-retinal space and can be observed apparently moving towards the recipient ONL, only small numbers succeed in integrating and differentiating into mature cone photoreceptors. The adult environment favoured the integration and differentiation of rods even when the majority of the transplanted population was destined to develop as cones in the developing retinal environment.

We then considered whether the immature retina favours new cone cell integration. Although retinal histogenesis in mice commences around mid-gestation, the retinal cell types and the associated circuitry are not fully assembled and mature until at least three weeks after birth. Immature cone

cells undergo an extensive migratory process within the nascent ONL between P9 and P20, first descending towards the inner nuclear layer (P9–P14) and then returning to the outer aspect of the ONL, where they assume their mature positions around the time of weaning (P20) (29). We reasoned that this dynamic environment may enhance the level of cone cell integration using CrxGFP donor cells. Transplantation of embryonic CrxGFP donor cells into immature pre-wean (P14) wild-type pups gave rise to similar overall number of integrated mature photoreceptors compared with adult recipients ($P = 0.107$). However, we found that the proportion of cones was not significantly increased suggesting that the immature environment is not more favourable for integration (Supplementary Material, Fig. S7A; median *Rxry*/GFP adult host = 0.361% and median P14 host 0.737%, $P = 0.105$; range of total number of integrated cones in P14 host = 0–22).

Cone and rod CrxGFP precursors integrate into the *Crb1*^{rd8/rd8} retina

Finally, we tested the efficacy of this new population of integration competent cells in two different models of LCA. Mutations in *CRB1*, a homologue of *Drosophila* Crumbs, cause severe retinal diseases such as LCA and retinitis pigmentosa in humans (30). *Crb1*^{rd8/rd8} mutant mice harbour a single base pair deletion in the *Crb1* gene, which results in a premature stop codon. As *Crb1* is required for maintenance of the outer limiting membrane (OLM), this structure is severely compromised in *Crb1*^{rd8/rd8} mice and the retina degenerates (31). Moreover, we recently showed that the OLM acts as a migration barrier for postnatal rod precursors. OLM disruption in *Crb1*^{rd8/rd8} mice or administration of the glial toxin DL-alpha-aminoadipic acid increases the rod integration levels in the ONL significantly (32,33). We thus reasoned that higher levels of cone cell integration may be achieved in the *Crb1*^{rd8/rd8} retina.

Three weeks after embryonic CrxGFP donor cells were transplanted into 6-week-old *Crb1*^{rd8/rd8} mice, large numbers of CrxGFP-positive precursors had migrated into the ONL of the host animals, and developed typical photoreceptor morphologies (Fig. 5A and B). Similar to wild-type recipients, the majority of integrated GFP-positive photoreceptors in *Crb1*^{rd8/rd8} retinæ displayed characteristics of mature rod cells. A trend of higher numbers of integrated photoreceptor cells was observed in the mutant retinæ (median = 1894) compared with wild-type controls (median = 508), though this difference did not meet the most stringent statistical criteria ($P = 0.052$; Fig. 5C). Previously, we found significantly increased integration levels of rod cells in the *Crb1*^{rd8/rd8} retina compared with wild-type following the transplantation of unsorted P4 donor cells (32). These differences likely reflect differences in the properties of the different age donor cell populations.

Analysis of treated *Crb1*^{rd8/rd8} eyes revealed GFP/*Rxry*-expressing cells, which displayed the characteristic morphology of cone cells (Fig. 5B). Therefore, we conclude that transplantation of embryonic CrxGFP donors leads to integration of new cones and rod photoreceptors in this model of LCA. Cone integration was not significantly different

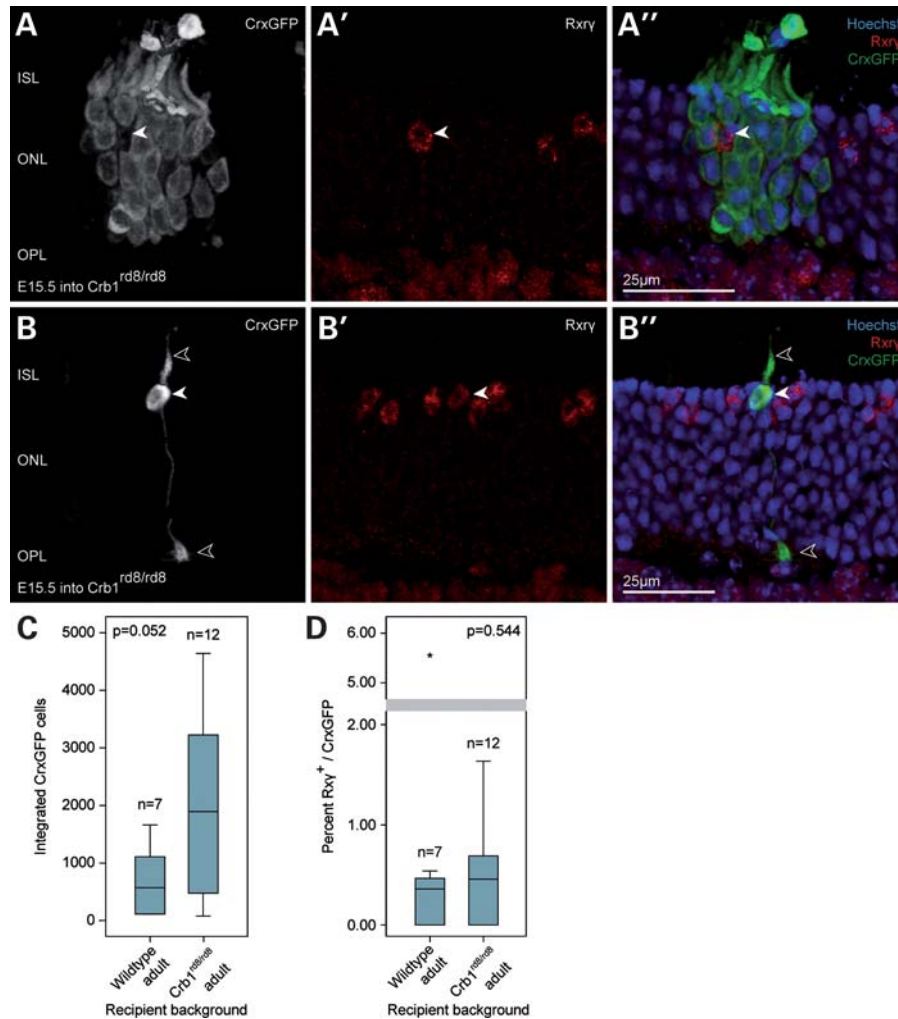


Figure 5. Transplantation of embryonic CrxGFP donor cells into the degenerating *Crb1^{rd8/rd8}* retina. (A) A cluster of transplanted CrxGFP rod photoreceptors (green) surrounding an Rxry-positive cone photoreceptor of the recipient retina (arrowhead). (B) Example of a transplanted CrxGFP cell exhibiting cone morphology (stubby inner segment, cone pedicle in the OPL, open arrowheads) and expressing the nuclear cone marker Rxry (solid arrowhead). (C) Comparison of the total number of integrated photoreceptors (rods and cones) after transplantation of E15.5 donor CrxGFP cells in the mutant and wild-type retina. Overall, photoreceptor integration was not significantly affected by the recipient environment (Mann–Whitney, $P = 0.052$). (D) Comparison of the cone integration efficiency (% Rxry/CrxGFP) of E15.5 CrxGFP cells in the mutant and wild-type retina. No statistically significant difference was observed (Mann–Whitney, $P = 0.544$). Horizontal bars indicate the median value. All retinas were examined 3 weeks post-transplantation. (A, B) are confocal z-projections. ISL, inner segment layer; ONL, outer nuclear layer; OPL, outer plexiform layer.

from the wild-type controls ($P = 0.544$), indicating that a disruption of the OLM alone does not preferentially enhance migration of this cell type from the sub-retinal space into the host ONL (Fig. 5D). These data indicate that the *Crb1^{rd8/rd8}* disease model presents at least an equivalent, if not a more favourable environment than the wild-type retina, for integration of new cone and rod photoreceptors.

Enhanced cone cell integration in the *Gucy2e*^{-/-} retina

Mutations in *GUCY2D*, the human homologue of the mouse *Gucy2e* gene, cause type 1a LCA characterized by rod–cone degeneration, while targeted deletion of the *Gucy2e* gene in mice results in cone dystrophy (34,35). Although cones develop and even elaborate outer segments in *Gucy2e*^{-/-} mice, they are non-functional and their numbers progressively

decline after 2–3 month of age (34). Rods, on the other hand, are affected to a lesser extent, retain light responsiveness and survive even long after most cones have degenerated.

In agreement with previous studies reporting cone loss, we observed a severe reduction of endogenous Rxry-expressing cone cells in 3-month-old *Gucy2e* knockout mice, while the rest of the ONL architecture was largely left intact (Supplementary Material, Fig. S8A and B). The overall number of cones found in the knockout retina was reduced to ~25% of that found in normal retinas of similar age (Supplementary Material, Fig. S5C). We hypothesized that in retinas with these alterations in photoreceptor organization, cues might exist that would facilitate the migration of transplanted cone precursors.

Following transplantation of embryonic CrxGFP donor cells into *Gucy2e* knockout mice, we observed comparable

numbers of integrated photoreceptors to wild-type recipients ($P = 0.286$; Fig. 6F). Immunostaining and morphological analysis confirmed cone identities (Fig. 6B–E). In this disease model, we found that cone cell integration was significantly increased ~ 13 -fold when compared with the wild-type ($P = 0.019$; Fig. 6G). Although the median contribution of cones to the total number of integrated photoreceptors in wild-type animals was $\sim 0.147\%$ (range of number of cones observed per retina = 0–10), we identified 1.912% (range of number of cones observed per retina = 2–28) in mice with cone dystrophy. Transplantation of precursors into P14 *Gucy2e* knockout mice resulted in similar levels of cone integration (range of number of cones observed per retina = 2–26). In this disease model, cone integration was readily observed in retinæ in which the number of integrated rod photoreceptors was low. Taken together, these data suggest that loss of cones and consequently disruption of the ratio of the two photoreceptor types in the recipient retina creates an environment that specifically benefits the migration of cone precursors. Notably, transplantation of the embryonic CrxGFP donor population gives rise to new integrated cones and rods in the disease model close to the normal murine cone to rod ratio of 1:35.

In conclusion, these studies show that the CrxGFP embryonic-stage donor cell population is effective for transplantation into two models of LCA and generates both cone and rod photoreceptors. In addition, the enhanced integration observed in the cone-deficient retinæ may be beneficial for cell-transplantation therapies.

DISCUSSION

Recently, we and others, provided evidence that replacing lost rod photoreceptors via sub-retinal cell transplantation may be a feasible treatment option for genetic retinal disease involving loss of photoreceptors (5,6,36,37). These findings contrasted with previous assumptions that the adult retina was a non-permissive environment for the integration of new photoreceptors and their incorporation into the existing retinal circuitry. This insight opened up promising new avenues towards the development of novel therapeutic approaches for conditions that currently lack effective treatment options.

Most of the focus of recent research efforts has been on rod cells because of the fact that they represent the most abundant cell type in the murine retina and one important conclusion has been that only post-mitotic yet immature rod precursors, but not retinal stem cells or mature photoreceptors are able to integrate in significant numbers into the ONL after transplantation (5). Having previously defined a suitable cell population for rod photoreceptor transplantation, we have now extended our investigation to cone cells, essential for human colour and high acuity vision.

Here, we have demonstrated in proof-of-principle experiments that embryonic-stage photoreceptor precursors, marked by the expression of a CrxGFP transgene, represent a population that can integrate efficiently into the normal and diseased retina after transplantation and generate new cone as well as rod photoreceptors. As the Crx transcription

factor is a critical determinant of the entire photoreceptor lineage, with expression in all post-mitotic photoreceptor cells, we were able to use the CrxGFP reporter to assess the integration competency of *Crx*-expressing precursors during different stages of retinal histogenesis.

We find that flow-sorted CrxGFP-expressing precursors display an increase in rod integration efficiency with progressing developmental age of the donor cells. This is consistent with our previous results in which rod cell transplants, delineated by *Nrl* expression, were most effective when unsorted neural retina donor cells were from the early postnatal period (5). The number of integrated rod photoreceptors observed following transplantation of the flow-sorted postnatal P3 CrxGFP population (median 5610; range per retina = 754–15 402) was around 10-fold higher than our earlier report transplanting unsorted P1 postnatal cells (300–1000 cells per retina) (5). Flow-sorting enriches the donor population for cells that integrate, such that 0.4–7.5% of the 200 000 transplanted CrxGFP cells effectively integrate. Future research will need to develop improved methods to isolate cells with integration potential in order to separate them from cells that remain in the sub-retinal space. The transplanted newly integrated rods in the current study exhibited the same morphological and immunohistochemical profiles and correct orientation in the host ONL as mature rods. We previously demonstrated that such cells are able to make functional synaptic connections and enhance light sensitivity in light-induced pupil constriction tests and extracellular field potential recordings from the ganglion cell layer, though we have not yet been able to increase the number of integrated cells to a high enough level to demonstrate significant function by electroretinogram.

The molecular mechanisms underpinning the observation that rod cell integration is much more efficient following transplantation of postnatal *Crx*-expressing donor cells compared with embryonic *Crx*-expressing donors remain to be elucidated. During retinal development, rod photoreceptors are generated in two distinct waves, with the first cohort of cells appearing around E17.5 and the second one following with some delay near P1 (38). There is evidence that, although these cells exit the cell cycle at different times, they synchronize before progressing in their developmental programme towards becoming mature rod photoreceptors. It is therefore conceivable that *Crx*-expressing precursors taken from embryonic time points, despite expressing key regulators of photoreceptor development, have not yet reached the appropriate maturation stage required for optimal rod integration.

After transplantation of embryonic-stage CrxGFP precursors, we consistently observed new integrated cone photoreceptors in the host ONL, expressing the appropriate molecular markers and displaying characteristic cone morphology, including cone pedicles and multifocal nuclear heterochromatin. This is, to our knowledge, the first comprehensive study of cone precursor cell transplantation in the murine retina. Two previous studies have transplanted mixed retinal cell populations of ES-derived cells or RPCs and observed instances of expression of cone opsin in transplanted cells. These studies have not counted the number of putative cones or demonstrated clear cone morphological features (6,7). Our observations that embryonic-stage

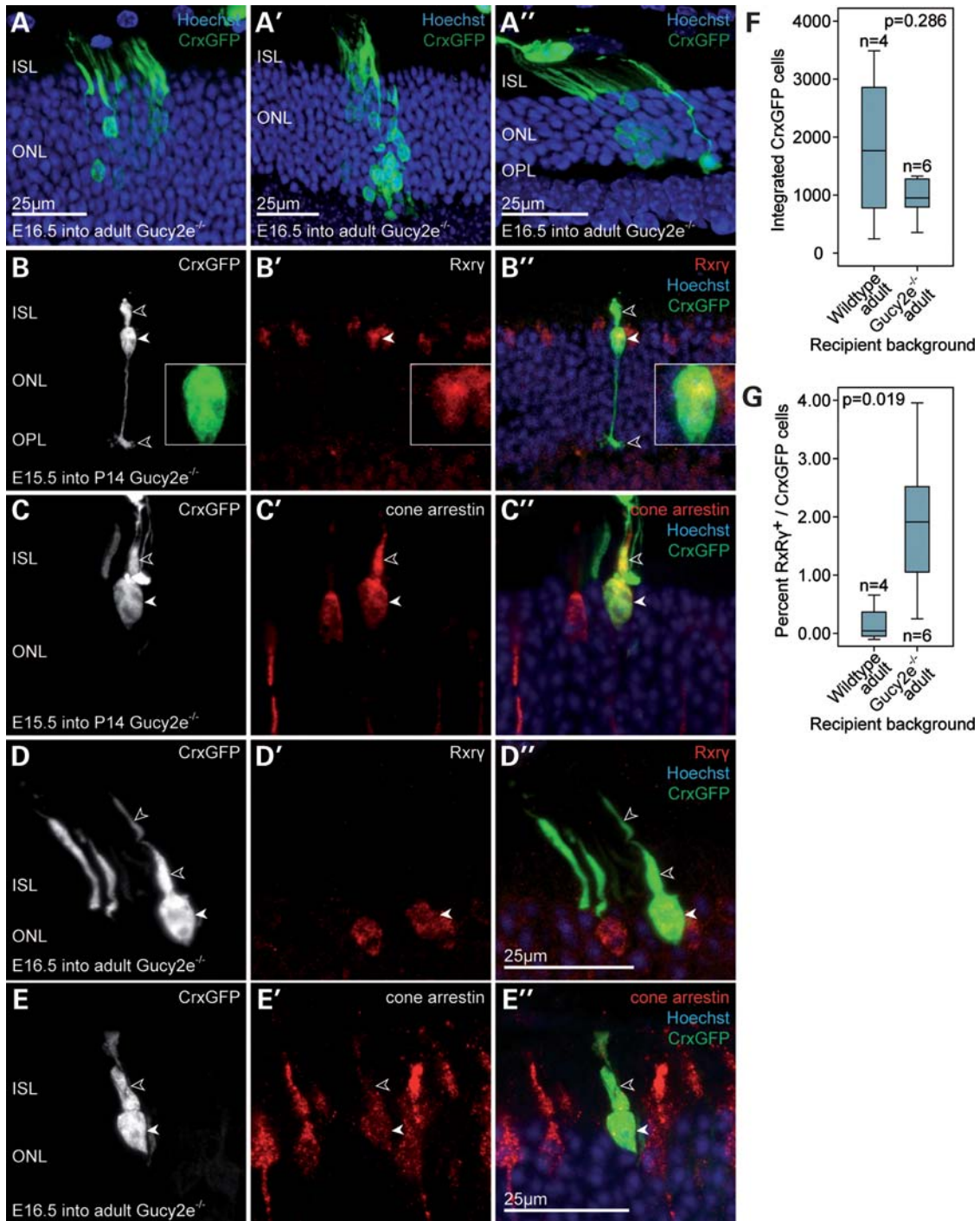


Figure 6. Transplantation of embryonic CrxGFP donor cells into the degenerating *Gucy2e*^{-/-} retina. (A–E) Embryonic CrxGFP donor cells transplanted into the *Gucy2e*^{-/-} degenerate retina at 2–3 months. (A) Transplanted CrxGFP donor cells exhibiting rod photoreceptor morphology after integrating into the ONL. (B–E) Examples of transplanted CrxGFP cells displaying cone morphology. (B,D) Cells express the nuclear cone marker Rxy (solid arrowheads and high magnification inset in B'). (C,E) Cone arrestin signal was observed in the inner segments and somata (open and solid arrowheads, respectively). (F) Comparison of the total number of integrated E16.5 CrxGFP photoreceptors (rods and cones) in the mutant and wild-type retina. Overall, photoreceptor integration was not significantly affected by the degenerative environment (Mann–Whitney, $P = 0.286$). Horizontal bars indicate the median value. All retinæ were examined 3 weeks post-transplantation. (A–E) are confocal z-projections. (G) Comparison of the cone integration efficiency (% Rxy/CrxGFP) of E16.5 CrxGFP cells in the mutant and wild-type retina. Cone integration was significantly more efficient after CrxGFP donor cell transplantation into the degenerating *Gucy2e*^{-/-} retina when compared with wild-type (Mann–Whitney, $P = 0.019$). ISL, inner segment layer; ONL, outer nuclear layer; OPL, outer plexiform layer.

Crx-positive donor cells generate cones, is in line with the important concept that donor cells having recently undergone terminal mitosis are appropriate for transplantation.

In the routine and reproducible observation of cones in our experiments (data from >70 transplants), their numbers were limited relative to the levels of rod cells observed. Maximal

cone integration efficiency was ~4% of the total new photoreceptors with the remainder being rod photoreceptors. It appears to be significant that the ratio of new cone to rods generated from transplanted CrxGFP donor cells remained similar to the 1:35 cone to rod ratio of photoreceptors normally present in the murine retina (39). The proportion of integrated Rrx γ /GFP-positive cone cells was much lower than the level of cone precursor cells present in the embryonic donor cell populations as indicated by Rrx γ staining, BrdU pulse chase experiments and classical photoreceptor cell birth-dating studies (12). It is not established when final specification to the cone fate occurs, however our data indicate that Rrx γ labels primarily cone precursors in the embryonic retina. As rod precursors make up an increasing percentage of Crx-positive cells with increasing developmental stage, the presumptive rods may interfere with cone integration and the more rods in the mix, the less cone integration. However, this could only provide a partial explanation, as in the embryonic-stage transplants, the number of new integrated cones is still lower than expected given the fact that the majority of cells transplanted were presumptive cones.

As transplanted CrxGFP cells readily differentiate as cone cells in the sub-retinal space, we have excluded the possibility that transplanted cone precursors do not survive after transplantation, though it is possible that cone precursors preferentially survive in the sub-retinal space. Rather than undergoing selective cell death, the transplanted embryonic post-mitotic cone precursor cells appear to have more limited migratory and integration abilities compared with the precursor population that develops into mature rods. Crx-positive cells have been shown to retain a degree of plasticity before they fully commit to becoming either of the two photoreceptor types (40–43), so it is possible that a proportion of presumed/fated cone cells in the embryonic CrxGFP donor population adopt a rod fate during migration into the adult ONL. The proportion of newly integrated cones and rods generated from the CrxGFP donors would then be determined during migration and differentiation in the host ONL. Our observations indicate that the adult retina is more permissive for rod integration compared with cone integration, and perhaps that the unidentified extrinsic mechanisms that determine the ratio of cone versus rod genesis from a common Crx-expressing precursor during development, may also act on the transplanted precursor cells within the host ONL. This mechanism would restrict the number of differentiating cones and determine the ratio of cone and rods in the retina.

Mouse models of retinal degeneration, especially those directly corresponding to human conditions involving loss of cones and rods, represent useful tools for the investigation of the effects of retinal cell transplantation and the potential therapeutic benefits. In this study, we evaluated the feasibility and efficacy of cone and rod photoreceptor transplantation in two such systems, the *Gucy2e* knock-out (35) and *Crb1* (31) mutant mice that model childhood retinal disease LCA.

Our data show that Crx-expressing precursors can indeed integrate into the degenerating retina at levels comparable to the wild-type retina. This is encouraging as efficient integration of transplanted cells is a prerequisite for any future therapeutic application of this technology. Furthermore, it

appears that cone cell integration is not solely a function of the intrinsic properties of the donor cells, but also depends on the host environment. When embryonic donor cells were transplanted into *Gucy2e* knockout mice, we observed that the proportion of integrated CrxGFP cells that differentiated into mature Rrx γ ⁺ cone cells was more than 10-fold higher when compared with the corresponding wild-type controls. These data raise the question of whether or not cone cell integration is specifically enhanced in the *Gucy2e*^{-/-} retinas, or perhaps integrated cells are directed to a cone cell fate by cues in the environment of these mutant retinas (both would increase the cone/rod ratio of integrated cells). The fact that an overall increase in the number of integrated cells was not observed even though E15.5 CrxGFP cells are mainly cone precursors favours the latter scenario. In contrast, transplantation of embryonic donor cells into mice lacking *Crb1* function, which is characterized by a reduced integrity of the OLM, did not result in a higher proportion of integrated cone cells. These results show that changes in the host environment can influence the integration efficiency of transplanted cone cells and importantly, in both models, degeneration at this stage does not reduce photoreceptor integration. These data lead us to speculate that alterations of the ONL composition, in particular, with respect to the cone distribution, are responsible for an increased proportion of integrated cones in the retinas of *Gucy2e*^{-/-} mice. Alternatively, it is possible that diffusible molecules secreted by the host retina are able to modulate the migration and integration behaviour of cone cells. In future work, it will be important to investigate the effect of different degenerative environments on donor cell behaviour and to perform long-term studies to investigate cell survival. Further molecular characterization of the defects in different mutants such as the *Crb1*^{rd8/rd8}, may also yield important information on optimizing transplant efficiency.

In summary, our proof-of-principle experiments clearly indicate that transplantation of cone as well as rod cells into the diseased retina is feasible. We consistently observed cone cell integration using embryonic-stage donors in wild-type and two different degenerating host retinas. Moreover, our data indicate that transplanted cells respond to the host environment and differentiate cone and rod cells in appropriate ratios similar to that of the host retina, with increased levels of cones developing after transplantation into the cone-deficient environment. The next challenge will be to develop novel approaches to increase the yield of photoreceptors, especially cones for transplantation. In this study, we have provided a starting point by defining the developmental stages of precursor cells that are competent for cone transplantation. As our knowledge of normal photoreceptor development advances, new genetic tools will become available that will greatly contribute to this end. Application of the current understanding of retinal development has already resulted in significant progress with respect to the generation of photoreceptors from either iPS cells or ES cells (44–48). In addition, the optimization of cell-delivery protocols as well as an increased understanding of the effects mediated by the host environment will facilitate improved integration efficiencies and hopefully lead to new treatment options for degenerative diseases of the retina in the future.

MATERIALS AND METHODS

Histology and immunohistochemistry

Retina were prepared, sectioned and immunostained as detailed in the Supplementary Material. Microscopy, image acquisition and processing are described in the Supplementary Material.

Retinal transplantations

Neural retinae were isolated from the CrxGFP transgenic mouse line (26) by micro-dissection. The CrxGFP-expressing cell population from a range of developmental stages (E13.5, E14.5, E15.5, E16.5, E17.5, P2 and P3) was isolated by fluorescent-activated cell sorting as detailed in the Supplemental Material.

Adult (defined as 6–8 weeks old) C57Bl/6J mice or *Gucy2e*^{-/-} (*RetGC1/GC-E*) (35) and *Crb1*^{rd8/rd8} (31) mutant mice were anaesthetized and 1 μ l of cell suspension (containing 200 000 sorted CrxGFP cells from each developmental stage) was injected into the sub-retinal space as described in the Supplemental Material. Recipient mice were sacrificed at 3 weeks after cell transplantation and their eyes treated for analysis.

Counts of integrated photoreceptors

To establish the number of integrated photoreceptor cells in recipient retinae, CrxGFP cells in the recipient ONL were counted in serial sections through the eye. CrxGFP cells with a cell body located within the ONL and displaying at least one of the following structures: inner/outer segment, synapse in the OPL, were scored as new photoreceptors. All transplanted eyes that contained more than one CrxGFP cell in the ONL were included in statistical analyses and all data points are represented in graphs. Mann–Whitney tests were performed to compare median integration efficiencies between samples. Spearman's bivariate analysis was performed to assess correlations between developmental age of donor cells and total number of integrated cells.

Cone integration efficiency

To assess the cone integration potential of CrxGFP donor cells, Rxr γ and GFP staining was counted. All sections were screened for integrated CrxGFP-positive cells in the ONL. Cells located at the outermost (scleral) edge of the ONL, showing a multifocal nuclear morphology, expressing Rxr γ and displaying one of the following: cone pedicle, inner and outer segments, were scored as new cone photoreceptors. By contrast, rod photoreceptors were recognizable by the absence of Rxr γ labelling, location of cell body within the ONL, and typical rod-condensed nuclear morphology and characteristic spherular rod synapse in the OPL. CrxGFP cell counts from alternate serial sections were doubled to extrapolate the total amount of integrated photoreceptors per eye. The cone integration efficiency for CrxGFP donor cells at each developmental stage was assessed by calculating the number of integrated cones as a percentage of the total number of integrated GFP-positive photoreceptors (double-labelled Rxr γ /CrxGFP-positive cells divided by the total number of integrated CrxGFP-positive cells). The number of rods was calculated by subtracting the number of cones from the total integrated CrxGFP-positive

cells. Mann–Whitney and Spearman's bivariate analysis were performed to compare and correlate cone integration efficiencies between samples.

Bromodeoxyuridine-labelling post-transplantation

Recipient mice received intra-peritoneal injections of BrdU (Sigma, 100 ng/g body weight) immediately following the transplantation and every day for the next 7 days. Eyes were processed and sectioned as described in the Supplemental Material.

SUPPLEMENTARY MATERIAL

Supplementary Material is available at *HMG* online.

ACKNOWLEDGEMENTS

We thank Constance Cepko for providing the CrxGFP mouse line; Krzysztof Palczewski for the RetGC1 (*Gucy2e*) antibody; Ulrich Luhmann for genotyping assistance, Angie Wade for statistical advice and the UCL Institute of Child Health flow cytometry and confocal facilities for technical support.

Conflict of Interest statement: The authors declare no competing interests with the work presented in this manuscript.

FUNDING

This work was supported by the Medical Research Council UK (G03000341 and G0901550); the Macula Vision Research Foundation; Fight for Sight; the Wellcome Trust (082217); the Ulverschroft Foundation; NIHR Biomedical Research Centre for Ophthalmology at Moorfields Eye Hospital and UCL Institute of Ophthalmology; NIHR Biomedical Research Centre for Paediatric Research at Great Ormond Street Hospital for Children and UCL Institute of Child Health. R.A.P. is a Royal Society University Research Fellow and J.W.B. is a Wellcome Advanced Fellow. Funding to pay the Open Access Charge was provided by the Wellcome Trust.

REFERENCES

- Morrow, E.M., Furukawa, T. and Cepko, C.L. (1998) Vertebrate photoreceptor cell development and disease. *Trends Cell Biol.*, **8**, 353–358.
- Hartong, D.T., Berson, E.L. and Dryja, T.P. (2006) Retinitis pigmentosa. *Lancet*, **368**, 1795–1809.
- Lamba, D.A., Karl, M.O. and Reh, T.A. (2009) Strategies for retinal repair: cell replacement and regeneration. *Prog. Brain Res.*, **175**, 23–31.
- West, E.L., Pearson, R.A., MacLaren, R.E., Sowden, J.C. and Ali, R.R. (2009) Cell transplantation strategies for retinal repair. *Prog. Brain Res.*, **175**, 3–21.
- MacLaren, R.E., Pearson, R.A., MacNeil, A., Douglas, R.H., Salt, T.E., Akimoto, M., Swaroop, A., Sowden, J.C. and Ali, R.R. (2006) Retinal repair by transplantation of photoreceptor precursors. *Nature*, **444**, 203–207.
- Lamba, D.A., Gust, J. and Reh, T.A. (2009) Transplantation of human embryonic stem cell-derived photoreceptors restores some visual function in *Crx*-deficient mice. *Cell Stem Cell*, **4**, 73–79.
- Klassen, H.J., Ng, T.F., Kurimoto, Y., Kirov, I., Shatos, M., Coffey, P. and Young, M.J. (2004) Multipotent retinal progenitors express developmental markers, differentiate into retinal neurons, and preserve light-mediated behavior. *Invest. Ophthalmol. Vis. Sci.*, **45**, 4167–4173.
- Turner, D.L. and Cepko, C.L. (1987) A common progenitor for neurons and glia persists in rat retina late in development. *Nature*, **328**, 131–136.

9. Turner, D.L., Snyder, E.Y. and Cepko, C.L. (1990) Lineage-independent determination of cell type in the embryonic mouse retina. *Neuron*, **4**, 833–845.
10. Marquardt, T. and Gruss, P. (2002) Generating neuronal diversity in the retina: one for nearly all. *Trends Neurosci.*, **25**, 32–38.
11. Cepko, C.L., Austin, C.P., Yang, X., Alexiades, M. and Ezzeddine, D. (1996) Cell fate determination in the vertebrate retina. *Proc. Natl Acad. Sci. USA*, **93**, 589–595.
12. Carter-Dawson, L.D. and LaVail, M.M. (1979) Rods and cones in the mouse retina. II. Autoradiographic analysis of cell generation using tritiated thymidine. *J. Comp. Neurol.*, **188**, 263–272.
13. Chen, S., Wang, Q.L., Nie, Z., Sun, H., Lennon, G., Copeland, N.G., Gilbert, D.J., Jenkins, N.A. and Zack, D.J. (1997) *Crx*, a novel *Otx*-like paired-homeodomain protein, binds to and transactivates photoreceptor cell-specific genes. *Neuron*, **19**, 1017–1030.
14. Hennig, A.K., Peng, G.H. and Chen, S. (2008) Regulation of photoreceptor gene expression by *Crx*-associated transcription factor network. *Brain Res.*, **1192**, 114–133.
15. Nishida, A., Furukawa, A., Koike, C., Tano, Y., Aizawa, S., Matsuo, I. and Furukawa, T. (2003) *Otx2* homeobox gene controls retinal photoreceptor cell fate and pineal gland development. *Nat. Neurosci.*, **6**, 1255–1263.
16. Koike, C., Nishida, A., Ueno, S., Saito, H., Sanuki, R., Sato, S., Furukawa, A., Aizawa, S., Matsuo, I., Suzuki, N. *et al.* (2007) Functional roles of *Otx2* transcription factor in postnatal mouse retinal development. *Mol. Cell Biol.*, **27**, 8318–8329.
17. Furukawa, T., Morrow, E.M. and Cepko, C.L. (1997) *Crx*, a novel *otx*-like homeobox gene, shows photoreceptor-specific expression and regulates photoreceptor differentiation. *Cell*, **91**, 531–541.
18. Peng, G.H., Ahmad, O., Ahmad, F., Liu, J. and Chen, S. (2005) The photoreceptor-specific nuclear receptor *Nr2e3* interacts with *Crx* and exerts opposing effects on the transcription of rod versus cone genes. *Hum. Mol. Genet.*, **14**, 747–764.
19. Mitton, K.P., Swain, P.K., Chen, S., Xu, S., Zack, D.J. and Swaroop, A. (2000) The leucine zipper of NRL interacts with the CRX homeodomain. A possible mechanism of transcriptional synergy in rhodopsin regulation. *J. Biol. Chem.*, **275**, 29794–29799.
20. Roberts, M.R., Hendrickson, A., McGuire, C.R. and Reh, T.A. (2005) Retinoid X receptor (gamma) is necessary to establish the S-opsin gradient in cone photoreceptors of the developing mouse retina. *Invest. Ophthalmol. Vis. Sci.*, **46**, 2897–2904.
21. Roberts, M.R., Srinivas, M., Forrest, D., Morreale de Escobar, G. and Reh, T.A. (2006) Making the gradient: thyroid hormone regulates cone opsin expression in the developing mouse retina. *Proc. Natl Acad. Sci. USA*, **103**, 6218–6223.
22. Hyatt, G.A. and Dowling, J.E. (1997) Retinoic acid. A key molecule for eye and photoreceptor development. *Invest. Ophthalmol. Vis. Sci.*, **38**, 1471–1475.
23. Sohocki, M.M., Sullivan, L.S., Mintz-Hittner, H.A., Birch, D., Heckenlively, J.R., Freund, C.L., McInnes, R.R. and Daiger, S.P. (1998) A range of clinical phenotypes associated with mutations in *CRX*, a photoreceptor transcription-factor gene. *Am. J. Hum. Genet.*, **63**, 1307–1315.
24. Freund, C.L., Gregory-Evans, C.Y., Furukawa, T., Papaioannou, M., Looser, J., Ploder, L., Bellingham, J., Ng, D., Herbrick, J.A., Duncan, A. *et al.* (1997) Cone-rod dystrophy due to mutations in a novel photoreceptor-specific homeobox gene (*CRX*) essential for maintenance of the photoreceptor. *Cell*, **91**, 543–553.
25. Furukawa, T., Morrow, E.M., Li, T., Davis, F.C. and Cepko, C.L. (1999) Retinopathy and attenuated circadian entrainment in *Crx*-deficient mice. *Nat. Genet.*, **23**, 466–470.
26. Samson, M., Emerson, M.M. and Cepko, C.L. (2009) Robust marking of photoreceptor cells and pinealocytes with several reporters under control of the *Crx* gene. *Dev. Dyn.*, **238**, 3218–3225.
27. Garelli, A., Rotstein, N.P. and Politi, L.E. (2006) Docosahexaenoic acid promotes photoreceptor differentiation without altering *Crx* expression. *Invest. Ophthalmol. Vis. Sci.*, **47**, 3017–3027.
28. Solovei, I., Kreysing, M., Lanctot, C., Kosem, S., Peichl, L., Cremer, T., Guck, J. and Joffe, B. (2009) Nuclear architecture of rod photoreceptor cells adapts to vision in mammalian evolution. *Cell*, **137**, 356–368.
29. Jia, L., Oh, E.C., Ng, L., Srinivas, M., Brooks, M., Swaroop, A. and Forrest, D. (2009) Retinoid-related orphan nuclear receptor RORbeta is an early-acting factor in rod photoreceptor development. *Proc. Natl Acad. Sci. USA*, **106**, 17534–17539.
30. den Hollander, A.I., Davis, J., van der Velde-Visser, S.D., Zonneveld, M.N., Pierrotet, C.O., Koenekoop, R.K., Kellner, U., van den Born, L.I., Heckenlively, J.R., Hoyng, C.B. *et al.* (2004) *CRB1* mutation spectrum in inherited retinal dystrophies. *Hum. Mutat.*, **24**, 355–369.
31. Mehalow, A.K., Kameya, S., Smith, R.S., Hawes, N.L., Denegre, J.M., Young, J.A., Bechtold, L., Haider, N.B., Tepass, U., Heckenlively, J.R. *et al.* (2003) *CRB1* is essential for external limiting membrane integrity and photoreceptor morphogenesis in the mammalian retina. *Hum. Mol. Genet.*, **12**, 2179–2189.
32. Pearson, R.A., Barber, A.C., West, E.L., MacLaren, R.E., Duran, Y., Bainbridge, J.W., Sowden, J.C. and Ali, R.R. (2010) Targeted disruption of outer limiting membrane junctional proteins (*Crb1* and *ZO-1*) increases integration of transplanted photoreceptor precursors into the adult wildtype and degenerating retina. *Cell Transpl.*, **19**, 487–503.
33. West, E.L., Pearson, R.A., Tschernutter, M., Sowden, J.C., MacLaren, R.E. and Ali, R.R. (2008) Pharmacological disruption of the outer limiting membrane leads to increased retinal integration of transplanted photoreceptor precursors. *Exp. Eye Res.*, **86**, 601–611.
34. Baehr, W., Karan, S., Maeda, T., Luo, D.G., Li, S., Bronson, J.D., Watt, C.B., Yau, K.W., Frederick, J.M. and Palczewski, K. (2007) The function of guanylate cyclase 1 and guanylate cyclase 2 in rod and cone photoreceptors. *J. Biol. Chem.*, **282**, 8837–8847.
35. Yang, R.B., Robinson, S.W., Xiong, W.H., Yau, K.W., Birch, D.G. and Garbers, D.L. (1999) Disruption of a retinal guanylyl cyclase gene leads to cone-specific dystrophy and paradoxical rod behavior. *J. Neurosci.*, **19**, 5889–5897.
36. Aftab, U., Jiang, C., Tucker, B., Kim, J.Y., Klassen, H., Miljan, E., Sinden, J. and Young, M. (2009) Growth kinetics and transplantation of human retinal progenitor cells. *Exp. Eye Res.*, **89**, 301–310.
37. Bartsch, U., Oriyakhel, W., Kenna, P.F., Linke, S., Richard, G., Petrowitz, B., Humphries, P., Farrar, G.J. and Ader, M. (2008) Retinal cells integrate into the outer nuclear layer and differentiate into mature photoreceptors after subretinal transplantation into adult mice. *Exp. Eye Res.*, **86**, 691–700.
38. Morrow, E.M., Belliveau, M.J. and Cepko, C.L. (1998) Two phases of rod photoreceptor differentiation during rat retinal development. *J. Neurosci.*, **18**, 3738–3748.
39. Jeon, C.J., Strettoi, E. and Masland, R.H. (1998) The major cell populations of the mouse retina. *J. Neurosci.*, **18**, 8936–8946.
40. Adler, R. and Hatlee, M. (1989) Plasticity and differentiation of embryonic retinal cells after terminal mitosis. *Science (New York, NY)*, **243**, 391–393.
41. Ezzeddine, Z.D., Yang, X., DeChiara, T., Yancopoulos, G. and Cepko, C.L. (1997) Postmitotic cells fated to become rod photoreceptors can be respecified by CNTF treatment of the retina. *Development (Cambridge, England)*, **124**, 1055–1067.
42. Nikonov, S.S., Daniele, L.L., Zhu, X., Craft, C.M., Swaroop, A. and Pugh, E.N. Jr. (2005) Photoreceptors of *Nrl*^{-/-} mice coexpress functional S- and M-cone opsins having distinct inactivation mechanisms. *J. Gen. Physiol.*, **125**, 287–304.
43. Oh, E.C., Khan, N., Novelli, E., Khanna, H., Strettoi, E. and Swaroop, A. (2007) Transformation of cone precursors to functional rod photoreceptors by bZIP transcription factor NRL. *Proc. Natl Acad. Sci. USA*, **104**, 1679–1684.
44. Osakada, F., Jin, Z.B., Hiram, Y., Ikeda, H., Danjyo, T., Watanabe, K., Sasai, Y. and Takahashi, M. (2009) *In vitro* differentiation of retinal cells from human pluripotent stem cells by small-molecule induction. *J. Cell Sci.*, **122**, 3169–3179.
45. Osakada, F., Ikeda, H., Sasai, Y. and Takahashi, M. (2009) Stepwise differentiation of pluripotent stem cells into retinal cells. *Nat. Protocols*, **4**, 811–824.
46. Hiram, Y., Osakada, F., Takahashi, K., Okita, K., Yamanaka, S., Ikeda, H., Yoshimura, N. and Takahashi, M. (2009) Generation of retinal cells from mouse and human induced pluripotent stem cells. *Neurosci. Lett.*, **458**, 126–131.
47. Osakada, F., Ikeda, H., Mandai, M., Wataya, T., Watanabe, K., Yoshimura, N., Akaike, A., Sasai, Y. and Takahashi, M. (2008) Toward the generation of rod and cone photoreceptors from mouse, monkey and human embryonic stem cells. *Nat. Biotechnol.*, **26**, 215–224.
48. Meyer, J.S., Shearer, R.L., Capowski, E.E., Wright, L.S., Wallace, K.A., McMillan, E.L., Zhang, S.C. and Gamm, D.M. (2009) Modeling early retinal development with human embryonic and induced pluripotent stem cells. *Proc. Natl Acad. Sci. USA*, **106**, 16698–16703.